Compressive Sensing Based Stochastic Economic Dispatch With High Penetration Renewables

Jing Li, Na Ou, Guang Lin, and Wei Wei

Abstract—**This paper develops a stochastic economic dispatch algorithm to optimize performance objectives while coping with high-dimensional uncertainty in the distribution system. To build a new convex deterministic optimization model of economic dispatch with random parameters, the conic relaxation of power flow and the multivariate polynomial chaos expansions of random variables are employed. As the expansion of the multivariate random variables in terms of polynomial bases are approximately sparse, the weighted l_1 minimization approach is utilized to reconstruct the polynomials from compressed samples. Based on the alternating direction method of multipliers, distributed strategy is developed to solve the economic dispatch and corresponding uncertainty quantification iteratively. Compared with Monte Carlo sampling method, the proposed approach not only can reduce the computational cost for solving stochastic economic dispatch, but also provide more accurate statistical information.**

Index Terms—**Compressive sensing, K-L expression, sparse polynomial approximation, uncertainty qualification, stochastic economic dispatch.**

I. Introduction

ECONOMIC dispatch (ED) is a such problem that it schedules the controllable units to minimize the overall production costs satisfying operational constraints in the electric power grid [1]. With the increasing number of Renewable Energy Sources (RES) based distributed generators (DGs) integrated in future distribution system, uncertainties are becoming a big issue in system operations and planning.

An alternative to deal with uncertainty is to a finite set of sampled realizations form a stochastic process model, thus the stochastic ED problem is handled to minimize the expected value of cost considering a set of scenarios [2]. Besides, chance constraint is a comprehensive way of handling uncertainty, and it is commonly used to ensure small probability of constraint violation [3]. While a sample based approach is used to handle the chanc constraint [4], computational tractability for large systems is still a challenge to be address. Especially, when uncertainties are sufficiently large, it fails to provide useful information. Reference [5] proposed a scalable robust multi-period DC-OPF integrating storage and uncertainty related to renewable generation. Whereas DC power flow models are lack of accuracy and unable to analysize voltage/reactive power, AC power flow is considered and convexified in the model [6]. Assuming that the forecast errors are small, partial linearization of AC power flow around the forecasted operating point is employed in [7]. And it proposes an analytical reformulation of chance constraint based on samples of random variables. In [8], the chance constrained AC-OPF (CC AC-OPF) is approximated by using data-driven distributionally robust optimization.

Some advanced modeling and sampling techniques from the field of uncertainty quantification (UQ) are adopted to the uncertainty analysis of many engineering problems including power system [9]. Spectral-method-based surrogate model is a powerful tool in studying UQ. Based on sparse grid interpolation [10] and Gaussian process models [11], it approximate the stochastic solution by a generalized polynomial-chaos (gPC) expansion [12]. Its representation of response surface is of a linear combination of orthonormal multivariate polynomials, and it can provide various statistical information [13] (e.g., moments and probability density function). However, computationally burden grows heavily with the number of data and dimension of random variables. Avoiding computationally expensive sampling, uncertainty propagation via general polynomial chaos expansion (gPC) is applied to solve stochastic OPF [14], [15], such that the single-period stochastic problem is reformulated as a structurally equivalent deterministic problem of larger dimension. Using Galerkin projection, the chance constraints are reformulated as second order cone constraints with gPC coefficients, and these coefficients are considered as auxiliary decision variables to be solved.

The intrusive method (e.g., stochastic Galerkin [16]) and non-intrusive method (e.g., probabilistic collocation method [17]) are the two mainly used approaches for approximating the gPC coefficients. Particularly, the non-intrusive method is widely used for the complex and nonlinear system as it does not need to modify the computational model of the system. However, there are lots of basis functions and simulation samples required for

Manuscript received April 13, 2018; revised August 7, 2018; accepted September 22, 2018. Date of publication October 8, 2018; date of current version February 18, 2019. This work was supported in part by Zhejiang Provincial Natural Science Foundation of China under Grant LQ15F030001, in part by key research and development projects in Zhejiang under Grant 2017C01039, and in part by National Science Foundation under Grants DMS-1555072 and DMS-1736364. Paper no. TPWRS-00531-2018. *(Corresponding author: Jing Li.)*

J. Li is with the Department of Information and Electrical Engineering, Zhejiang University City College, Hangzhou 310015, China, and the Department of Information and Electronic Engineering, Zhejiang Gongshang University, Hangzhou 310018, China (e-mail: eejing@zju.edu.cn).

N. Ou is with the College of Mathematics and Econometrics, Hunan University, Changsha 410082, China (e-mail: oyoungla@hnu.edu.cn).

G. Lin is with the Department of Mathematics, Purdue University, West Lafayette, IN 47907 USA (e-mail: guanglin@purdue.edu).

W. Wei is with the Department of Electrical Engineering, Zhejiang University, Hangzhou 310015, China (e-mail: wwei@zju.edu.cn).

Color versions of one or more of the figures in this paper are available online at http://ieeexplore.ieee.org.

Digital Object Identifier 10.1109/TPWRS.2018.2874718

problems with high-dimensional uncertainties. Some techniques based on compressed sensing [18], reduced basis [19], low rank decomposition [20] have been developed for high-dimensional problem.

Compressive-sensing-based uncertainty quantification methods [21], [22] have become a powerful tool for problems with limited data. When the number of zero terms in the gPC of the model output is big, the l_1 minimization method has approximated gPC coefficients from small number of and possibly arbitrarily positioned samples [23]. The sparsity improvement increases not only efficiency but also accuracy of the compressive sensing method.

In this paper, we adopt compressive sensing method from the field of UQ and leverage it to impact stochastic economic dispatch of power system. The proposed stochastic economic dispatch problem is modeled based on a multi-period optimal power flow formulation, chance constraints are formulated to ensure voltage regulation within given limits with arbitrarily high probability. Increasing penetration of RES based DGs brings a large number of uncertainties in the power system, the nonlinearity of optimal power equations and probabilistic constraints make the problem computationally intractable. However, the sparse gPC expansion is implemented in conjunction with the novel Karhunen-Loeve expansion (KLE) model of the stochastic renewable power generation, and the conic relaxation of power flow is employed to get the convex deterministic optimization model of economic dispatch problem with uncertainty. With help of gPC approximation, the chance constraints are represented by the conic constraints of polynomial coefficients. Additionally, a novel method for high-dimensional approximation based on compressed sensing techniques is developed under limited samples situation. Finally, a distributed strategy is developed by using the alternating direction method of multipliers (ADMM), to enable economic dispatch and compressive sensing based uncertainty quantification pursue specific performance objectives. Simulations verify that the proposed approach has high efficiency and accuracy for solving stochastic economic dispatch problem with high-dimensional uncertainty.

The contributions of our study are as follows:

- In our manuscript, the stochastic economic dispatching problem is formulated as a multi-period CC AC-OPF subject to the multiple period uncertainty in terms of stochastic process over a finite optimization horizon. With truncated Karhunen-Love expansion (KLE), the input multiple stochastic processes are parameterized in a reduced dimensional stochastic space.
- To break the curse of dimensionality, we build sparse gPC approximation of the multi-period CC AC-OPF upon the reformulation proposed in [14]. Under limited samples situation, the weighted L-1 minimization approach is utilized to reconstruct the gPC from compressed samples.
- Robust optimization seeks strategies that perform best with respect to the worst-case realization in the uncertainty set. Nevertheless, the proposed method in our manuscript not only obtain the optimal strategy but also give more statistic information of variables and objectives under uncertainty.

II. Preliminary

A. Representation of Power Flow

A distribution system generally has radial topology, which can be described by a directed tree graph $\boldsymbol{G} = (\boldsymbol{E}, \boldsymbol{\Omega})$, where $\boldsymbol{E} := \{n_0, n_1, \ldots, n_m\}$ denotes the vertex set representing the nodes(buses), $\boldsymbol{\Omega} := \{\omega_1, \omega_2, \ldots, \omega_m\}$ is the edge set. $\omega_j = \{(n_i, n_j) | n_i \in \boldsymbol{E}, n_j \in \boldsymbol{E} \setminus \{n_0\}\}$ denotes the line circuit from bus n_i to bus n_j. The root node n_0 denotes the substation bus in the distribution system which has fixed voltage V_0. In order to describe the relationship of edges and nodes, we construct the matrix A, the incidence matrix of the directed tree graph $\boldsymbol{G}' = \big(\boldsymbol{N} \setminus \{n_0\}, \boldsymbol{\Omega}\big)$ such that the elements of matrix A_{ij} are given as follows:

$$\mathrm{A}_{ij} = \begin{cases} +1 & \text{if } n_i \text{ is the child node of } \omega_j, \\ -1 & \text{if } n_i \text{ is the parent node of } \omega_j, \\ 0 & \text{otherwise.} \end{cases} \tag{1}$$

Let t denotes specific time periods in the planning horizon $t \in \mathcal{T}, \mathcal{T} = \{1, \ldots, T\}$. For jth branch in the distribution system at time t, let $I_j(t)$ be the complex current from buses $n_{\pi(j)}$ to n_j, $P_j(t)(Q_j(t))$ be the sending-end active (reactive) power from buses $n_{\pi(j)}$ to n_j, and $R_j(X_j)$ be the resistance (reactance) on the line from buses $n_{\pi(j)}$ to n_j. For each bus at time t, let $V_j(t)$ be the complex voltage on bus n_j, $p_j(t)(q_j(t))$ be the injected active (reactive) power on bus n_j.

Let, $v_j(t) := |V_j(t)|^2$, $l_j(t) := |I_j(t)|^2$. Based on the branch model of power flow [24], that is

$$\begin{bmatrix} \mathrm{A} & 0 & -\mathrm{R} & 0 \\ 0 & \mathrm{A} & -\mathrm{X} & 0 \\ 2\mathrm{R} & 2\mathrm{X} & -\mathrm{Z} & \mathrm{A}^T \end{bmatrix} \begin{bmatrix} \boldsymbol{P}(t) \\ \boldsymbol{Q}(t) \\ \boldsymbol{l}(t) \\ \boldsymbol{v}(t) \end{bmatrix} = \begin{bmatrix} \boldsymbol{p}(t) \\ \boldsymbol{q}(t) \\ v_0 \boldsymbol{e}_1 \end{bmatrix} \tag{2}$$

$$l_j(t) v_{\pi(j)}(t) = P_j^2(t) + Q_j^2(t); \quad \forall j \in \boldsymbol{\Omega}. \tag{3}$$

where for any given $(\boldsymbol{p}(t), \boldsymbol{q}(t))$, the state variables $\boldsymbol{S}(t) := [\boldsymbol{P}(t), \boldsymbol{Q}(t), \boldsymbol{l}(t), \boldsymbol{v}(t)]^T$ of the distribution system can be determined by above equations.

B. Nodal Power Injection

The nodal power injections are the power consumed by load minus the sum of the electric power power export of the renewable-based generator $\boldsymbol{p}^r(\xi, t)$ and the power of energy storage system $\boldsymbol{p}^b(t)$.

$$\boldsymbol{p}(t) = \boldsymbol{p}^d(t) + \boldsymbol{p}^{cd}(t) - \boldsymbol{p}^b(t) - \boldsymbol{p}^r(\xi, t). \tag{4}$$

where $\boldsymbol{p}^d(t)$ and $\boldsymbol{p}^{cd}(t)$ denote the uncontrollable and controllable load respectively. The reactive power is

$$\boldsymbol{q}(t) = \boldsymbol{q}^r(t) - \boldsymbol{q}^d(t). \tag{5}$$

where $\boldsymbol{q}^r(t)$ and $\boldsymbol{q}^d(t)$ denote the reactive power of generation and load respectively.

1) Uncertainty of Renewable Power: the renewable-based generation referred to as the available active power, that is given by

$$p_j^r(\xi,t) = \bar{p}_j^r(t) + err_j(\xi,t), \quad j \in \boldsymbol{E}^G, t \in \mathcal{T} \tag{6}$$

where $\boldsymbol{E}^G$ is the set of generator bus, $\bar{p}^r(t)$ is the forecast value of jth generator at time t and $err_j(\xi,t)$ is the error associated with the forecast . Motivated by the techniques of short-term forecast over the dispatching horizon [25], the forecast error is assumed to be modeled by stochastic process/random field. Applying the Karhunen-Loève expansion (KLE), the random field can be characterized by finite dimensional random space [26]. Considering the correlations between the multiple random fields $err_j(j \in \boldsymbol{E}^G)$, the covariance matrix $\boldsymbol{O}$ with the element

$$O_{ij} = \mathbb{E}[err_i(\xi,t)err_j(\xi,t)] \tag{7}$$

And then the covariance matrix is decomposed into $\boldsymbol{O} = \boldsymbol{L}\boldsymbol{L}^T$ by Cholesky decomposition. Incorporating the correlation into the representation of the input forecast error $err_j(j \in \boldsymbol{E}^G)$, the KLE of the multiple random fields is as follows:

$$err_j(\xi,t) \approx err_j^M(\xi,t) = \sigma_{err_j}\left(\sum_{k=1}^{j} l_{jk}\sum_{i=1}^{M}\sqrt{\mu_{i,k}}f_{i,k}(t)\xi_{i,k}\right) \tag{8}$$

where M is the number of KLE terms. σ_{err_j} is the standard deviation of err_j. μ_i and $f_i(t)$ is eigenvalue and corresponding eigenfunctions obtained by the spectral decomposition of covariance kernel of the stochastic process describing the forecast error of renewable generation at jth bus.

Here, it is assumed that the forecast error is approximately described by a Gaussian field [27]. Accordingly, we can simulate the stochastic process of error with a truncated KLE representation. Motivated by the analysis and empirical evidence for a real life example [28], [29], the normality assumption of the forecast error is justified. The normality assumption of the forecast error indicates that, in Eq. (8) $\{\xi_{i,k}\}_{i=1,\ldots,M,k\in\boldsymbol{E}^G}$ is a set of standard identically independent Gaussian random variables.

Remark 1: For non-gaussian processes, higher-order statistics should be considered. Nonlinear generation of KLE, which is known as kernel principal component analysis with high order polynomial kernels [30], [31], have been applied to handle non-gaussian process. Yet, the approach we proposed in our manuscript based on gaussian process of forecast error is general enough to be applicable with non-gaussian stochastic processes.

2) Model of Energy Storage System (ESS): The ESS can be considered as either a generator when it is discharged or a load when it is charged. At jth bus in the distribution system, let $B_j(t)$ denote the amount of energy storage at time $t \in \mathcal{T}$. Approximately,

$$B_j(t) = B_j(t-1) + p_j^b(t)\delta_\tau. \tag{9}$$

where $p_j^b(t)$ denotes the power delivered to or drawn from the ESS and δ_τ is the duration of time slot $(t, t+1]$. Particularly, $p_j^b(t)$ could be either charging or discharging power of ESS, it can be controlled and optimized.

Considering the effect on the cycle life of storage device, the operational limits of the storage device are as follows:

$$B_j(t) \in \left[B_j^{\min}, B_j^{\max}\right], \quad p_j^b(t) \in \left[p_j^{b\min}, p_j^{b\max}\right] \tag{10}$$

where $(B_j^{\min}, B_j^{\max})$ denotes the lower and upper bounds on energy level at jth bus. Here, it is assumed that they are 20% and 90% of the installed capacity of the storage units, respectively. And $(p_j^{b\min}, p_j^{b\max})$ denotes nominal discharging and charging rate of battery at jth bus respectively.

C. Uncertainty Quantization Via Stochastic Collocation

1) Generalized Polynomial Expansions: The uncertainties of injected power further influence the state variable such as bus voltage and branch current in power system. Given the d-dimensional random variables $\boldsymbol{\xi} = (\xi_1, \xi_2, \ldots, \xi_d)$. Obviously $\boldsymbol{S}(t)$ depends on $\boldsymbol{\xi}$ and thus can be approximated by a truncated generalized polynomial-chaos (gPC) expansion

$$\boldsymbol{S}(\boldsymbol{\xi},t) \approx \boldsymbol{S}^o(\boldsymbol{\xi},t) = \sum_{\alpha\in\Lambda_{o,d}} \tilde{\boldsymbol{S}}_\alpha(t)\boldsymbol{\phi}_\alpha(\boldsymbol{\xi}) \tag{11}$$

in which $\Lambda_{o,d} := \{\alpha \in \mathbb{N}_0^d : \sum_{i=1}^d \alpha_i \le o, \|\alpha\|_0 \le d\}$ is the set of multi-indices and has the cardinality $|\Lambda_{o,d}| = \frac{(o+d)!}{o!d!}$. And the multivariate polynomial basis function $\boldsymbol{\phi}_\alpha(\boldsymbol{\xi})$ is a tensor product of univariate polynomials $\phi_{\alpha_i}(\xi_i)$, i.e.,

$$\boldsymbol{\phi}_\alpha(\boldsymbol{\xi}) = \phi_{\alpha_1}(\xi_1)\phi_{\alpha_2}(\xi_2)\cdots\phi_{\alpha_d}(\xi_d), \quad \alpha \in \mathbb{N}_0^d \tag{12}$$

where $\mathbb{N}_0^d := \{(\alpha_1,\ldots,\alpha_d) : \alpha_i \in \mathbb{N}\cup\{0\}\}$ is the set of multi-indices of size d defined on non-negative integers. Each family of polynomials corresponds to a given choice of distribution for the ξ_i, such as normal distribution with Hermite polynomials, uniform with Legendre polynomials [32].

Then the expectation and variance are approximated by

$$\mathbb{E}[\boldsymbol{S}(\boldsymbol{\xi},t)] \approx \tilde{\boldsymbol{S}}_0(t), \quad \left(\mathrm{var}[\boldsymbol{S}(\boldsymbol{\xi},t)]\right)^2 \approx \sum_{i=1}^{N} \tilde{\boldsymbol{S}}_i^2(t) \tag{13}$$

where $N = |\Lambda_{o,d}| - 1$.

As $\boldsymbol{\phi}_\alpha(\boldsymbol{\xi})$ are orthonormal to each other, the exact gPC coefficients $\tilde{\boldsymbol{S}}(t)$ may be computed by Galerkin projection such that

$$\tilde{\boldsymbol{S}}_\alpha^\sharp(t) = \int_\Xi \boldsymbol{S}(\boldsymbol{\xi},t)\boldsymbol{\phi}_\alpha(\boldsymbol{\xi})\rho(\boldsymbol{\xi})d\boldsymbol{\xi} \tag{14}$$

where $\rho(\boldsymbol{\xi})$ is the distribution function of random $\boldsymbol{\xi}$.

2) Sparse gPC Approximation: The sparse gPC approximation $\widehat{\boldsymbol{S}}(\boldsymbol{\xi},t) := \sum_{\alpha\in\widehat{\Lambda}_{o,d}} \tilde{\boldsymbol{S}}_\alpha(t)\boldsymbol{\phi}_\alpha(\boldsymbol{\xi})$ is said that one may ideally seek a proper index set $\widehat{\Lambda}_{o,d} \subseteq \Lambda_{o,d}$, with sufficiently large order o, such that for a given accuracy δ

$$\Lambda_{o,d}^\delta := \arg\min\Big\{|\widehat{\Lambda}_{o,d}| : \widehat{\Lambda}_{o,d} \subseteq \Lambda_{o,d}, \left\|\boldsymbol{S}(\boldsymbol{\xi},t) - \widehat{\boldsymbol{S}}(\boldsymbol{\xi},t)\right\|_2 \le \delta\Big\} \tag{15}$$

where $|\Lambda_{o,d}^\delta| \ll |\Lambda_{o,d}|$ is the sparse index set.

III. Economic Optimization and Uncertain Quantization

In this section, the economic optimization of DGs is modeled by the chance-constrained stochastic programming formulation that the renewable power uncertainty is considered as the random inputs. For the random inputs are approximated by gPC, we explore the convex approximation of the thicky chance constraints and efficient representation of uncertainty for the economic optimization problem.

A. Model of Stochastic Optimization

Considering the stochastic modeling of RESs' behavior, the complete model materializes into a stochastic nonlinear optimization problem (SNO). Its objective is determining the minimum overall cost of operating the controllable resources and minimum power losses across all time periods t in the optimization horizon $\mathcal{T}$, subject to a certain number of constraints including chance constraints, as follows:

1) Objective Function: In this work, $\boldsymbol{u}(t) := (\boldsymbol{p}^b(t), \boldsymbol{p}^{cd}(t))^T$ is the design variable which includes the power of battery and controllable load. Concerning the branch power flow model in Eq. (2) and (3), the state variables can be specified for any given design variable. As a result of the random error $\boldsymbol{\xi}$ to the prediction of renewable energy, the state variables $\boldsymbol{S}(\boldsymbol{\xi},t) = [\boldsymbol{P}(\boldsymbol{\xi},t), \boldsymbol{Q}(\boldsymbol{\xi},t), \boldsymbol{l}(\boldsymbol{\xi},t), \boldsymbol{v}(\boldsymbol{\xi},t)]^T$ of the power system are random, and the power losses is stochastic as well.

Therefore, the optimal variables of the proposed DOPT are design variable $\boldsymbol{u}(t)$ and state variable $\boldsymbol{S}(\boldsymbol{\xi},t)$, and the objective function includes two parts: the expected value of power losses and the cost of operating controllable resources in the system, that is

$$\begin{aligned}\min \quad & \mathbb{E}_{\boldsymbol{\xi}\in\Xi}\left[\sum_{t\in\mathcal{T}} f_l(\boldsymbol{S}(\boldsymbol{\xi},t), \boldsymbol{u}(t))\right] \\ &= \sum_{t\in\mathcal{T}} \left(\mathbb{E}_{\boldsymbol{\xi}\in\Xi}\left[\Sigma_{j\in\Omega} R_j l_j(\boldsymbol{\xi},t)\right] + \rho_b \boldsymbol{p}^b(t) + \rho_d \boldsymbol{p}^{cd}(t)\right)\end{aligned} \tag{16}$$

where $E_{\boldsymbol{\xi}\in\Xi}$ is the expected value operator and Ξ is the space of random $\boldsymbol{\xi}$; ρ_d and ρ_b is unit cost of controllable load curtailment and unit battery cost respectively.

2) Power Balance Contraints: Considering the branch power flow equalities mentioned above in Eq. (2)~(3), these equalities constraints can be conically relaxed by the intersection of the affine set,

$$\mathrm{C}\boldsymbol{S}(\boldsymbol{\xi},t) = \mathrm{b}_t + \boldsymbol{u}(t) + \mathrm{a}_t\boldsymbol{\xi}; \tag{17}$$

and the second order cone,

$$l_j(\boldsymbol{\xi},t) v_{\pi(j)}(\boldsymbol{\xi},t) \geq P_j^2(\boldsymbol{\xi},t) + Q_j^2(\boldsymbol{\xi},t); \quad \forall j \in \boldsymbol{\Omega}. \tag{18}$$

which is the conic relaxed constraint of Eq. (3).

The matrix C is the constant matrix describing the relationship of the voltage, current and power in the power system.

$$\mathrm{C} = \begin{pmatrix} \mathrm{A} & 0 & -\mathrm{R} & 0 \\ 0 & \mathrm{A} & -\mathrm{X} & 0 \\ 2\mathrm{R} & 2\mathrm{X} & -\mathrm{Z} & \mathrm{A}^T \end{pmatrix} \tag{19}$$

And the constant $\mathrm{b}_t = [\bar{\boldsymbol{p}}^r(t) - \boldsymbol{p}^d(t), \boldsymbol{q}(t), v_0\boldsymbol{e}_1]^T$ denotes the given value, which includes the predicted power of RES, demand power and the voltage at slack bus in the distribution system.

In our proposed economic dispatching problem, the KLE is performed to approximate the multiple input stochastic processes (as shown in Eq. (8)). Let $\boldsymbol{\xi} := [\xi_{1,1}, \ldots, \xi_{M,1}, \xi_{1,2}, \ldots, \xi_{M,2}, \ldots, \xi_{M,N_g}]^T$ be the $M \times N_g$-dimensional random variables of the stochastic optimization problem. The constant matrix a_t is also given once the KLE approximation settled down, that is,

$$\mathrm{a}_t = \boldsymbol{\sigma_{err}} \boldsymbol{L} \boldsymbol{\varphi}(t) \tag{20}$$

where $\boldsymbol{\sigma_{err}} := [\sigma_{err_1}, \ldots, \sigma_{err_{N_g}}]$. $\boldsymbol{L}$ is a lower triangular matrix obtained by Cholesky decomposition of covariance matrix $\boldsymbol{O}$ with ijth element given in Eq. (7). And the matrix $\boldsymbol{\varphi}(t)$ is a block diagonal matrix,

$$\boldsymbol{\varphi}(t) = \begin{pmatrix} \boldsymbol{\varphi}_1(t) & 0 & \cdots & 0 \\ 0 & \boldsymbol{\varphi}_2(t) & & 0 \\ \vdots & & \ddots & \\ 0 & 0 & & \boldsymbol{\varphi}_{N_g}(t) \end{pmatrix} \tag{21}$$

where $\boldsymbol{\varphi}_j(t) := [\sqrt{\mu_{1,j}} f_{1,j}(t), \ldots, \sqrt{\mu_{M,j}} f_{M,j}(t)]$ is an $1 \times M$ row vector that given by the spectral decomposition of stochastic forecast error of renewable generation at j-th bus.

Remark 2: The inequality (18) is given by the conic relaxation of the branch power flow (3). For radial network, a branch flow model has been studied and relaxed, [33]–[35] prove a variety of sufficient conditions under which the optimal power flow is solved via second-order cone programming technique and the conic relaxation is exact. Here, it is assumed that both real and reactive power flow unidirectionally for all branches in the distribution system. According to the Proposition 2 in [34] and the prove of Theorem in [35], the conic relaxation of AC power flow in the proposed optimization model is feasible.

3) Control Limits: The controllable load and battery utilization over the whole horizon is optimized subject to the following constraints:

$$\boldsymbol{u}(t) \in [\underline{\mathrm{u}}, \overline{\mathrm{u}}], \quad \sum_{\tau=1}^{t} \boldsymbol{u}(\tau) \in [\underline{\mathrm{B}}, \overline{\mathrm{B}}] \tag{22}$$

where $[\underline{\mathrm{u}}, \overline{\mathrm{u}}]$ is the lower and upper bound of the design variable, it means that the power of battery and controllable load should be optimally designed within certain range. $[\underline{\mathrm{B}}, \overline{\mathrm{B}}]$ denotes the lower and upper bounds on energy level of battery (see (10)).

4) Chance Constraints: Given the predicted values of available renewable powers along with the associated forecasting errors $\boldsymbol{\xi}$, the RES based DGs and battery setpoints can be scheduled in a way that the limits of branch current and bus voltage are satisfied with prescribed probabilities $1-\epsilon$ [36]. The limits of bus voltages and branch currents are modeled as chance constraints:

$$\text{Prob}\left\{\boldsymbol{v}(\boldsymbol{\xi},\boldsymbol{t}) \leq \overline{\mathrm{v}}\right\} \geq 1-\epsilon; \tag{23a}$$

$$\text{Prob}\left\{\boldsymbol{v}(\boldsymbol{\xi},\boldsymbol{t}) \geq \underline{\mathrm{v}}\right\} \geq 1-\epsilon; \tag{23b}$$

$$\text{Prob}\left\{\boldsymbol{l}(\boldsymbol{\xi},\boldsymbol{t}) \leq \overline{\mathrm{l}}\right\} \geq 1-\epsilon. \tag{23c}$$

where $\bar{\mathrm{I}}$ denotes the the upper bound of the magnitude of branch currents. $[\underline{\mathrm{v}}, \overline{\mathrm{v}}]$ is the bound which the magnitude of voltage should be stay with.

Regarding the optimization problem (16)∼(23), it is the stochastic multi-period OPF problem in which the chance constraints make the problem intractable in high-dimensional cases. Applying surrogate model of uncertainties with the help of the gPC, a convex approximation of the chance constraints is proposed next.

B. Convex Approximation of Chance Constraints

The chance constraints like Eq. (23) are often nonconvex and difficult to treat in general, these constraints can be reformulated using the same approach as in [37]. Under some distributional assumptions for $\boldsymbol{v}(\boldsymbol{\xi}, \boldsymbol{t})$ and $\boldsymbol{l}(\boldsymbol{\xi}, \boldsymbol{t})$, the reformulation of chance constraint Eq. (23) is as the following analytic expression:

$$\mathbb{E}[\boldsymbol{v}(\boldsymbol{\xi}, t)] \leq \overline{\mathrm{v}} - f^{-1}(1-\epsilon)\mathrm{var}[\boldsymbol{v}(\boldsymbol{\xi}, t)]; \tag{24a}$$

$$\mathbb{E}[\boldsymbol{v}(\boldsymbol{\xi}, t)] \geq \underline{\mathrm{v}} + f^{-1}(1-\epsilon)\mathrm{var}[\boldsymbol{v}(\boldsymbol{\xi}, t)]; \tag{24b}$$

$$\mathbb{E}[\boldsymbol{l}(\boldsymbol{\xi}, t)] \leq \bar{\mathrm{I}} - f^{-1}(1-\epsilon)\mathrm{var}[\boldsymbol{l}(\boldsymbol{\xi}, t)]. \tag{24c}$$

where f^{-1} is the inverse cumulative distribution function of the standard normal distribution if the fluctuations of $\boldsymbol{v}(\boldsymbol{\xi}, \boldsymbol{t})$ and $\boldsymbol{l}(\boldsymbol{\xi}, \boldsymbol{t})$ follow normal distribution. It is possible to accounted for more general distribution without significant changes to the approach [38].

Additionally, the gPC is utilized as a surrogate model to understand the influence of uncertainties on the quantity of state variables in the distribution system, that is

$$\boldsymbol{v}(\boldsymbol{\xi}, t) = \sum_{i=0}^{N} \tilde{\boldsymbol{v}}_i(t)\phi_i(\boldsymbol{\xi}); \quad \boldsymbol{l}(\boldsymbol{\xi}, t) = \sum_{i=0}^{N} \tilde{\boldsymbol{l}}_i(t)\phi_i(\boldsymbol{\xi}) \tag{25}$$

Thus, the expected value and variance of random variables can be described by the coefficient of their gPC,

$$\mathbb{E}[\boldsymbol{v}(\boldsymbol{\xi}, t)] = \tilde{\boldsymbol{v}}_0(t), \quad \mathrm{var}[\boldsymbol{v}(\boldsymbol{\xi}, t)] = \sqrt{\sum\nolimits_{i=1}^{N} \tilde{\boldsymbol{v}}_i^2(t)}; \tag{26a}$$

$$\mathbb{E}[\boldsymbol{l}(\boldsymbol{\xi}, t)] = \tilde{\boldsymbol{l}}_0(t), \quad \mathrm{var}[\boldsymbol{l}(\boldsymbol{\xi}, t)] = \sqrt{\sum\nolimits_{i=1}^{N} \tilde{\boldsymbol{l}}_i^2(t)}. \tag{26b}$$

Substituting (26) into (24), the chance constraints Eq. (24) can be further represented as convex constraints of gPC coefficients.

$$\overline{\mathrm{v}} - \tilde{\boldsymbol{v}}_0(t) \geq f^{-1}(1-\epsilon)\sqrt{\tilde{\boldsymbol{v}}_1^2(t) + \cdots + \tilde{\boldsymbol{v}}_N^2(t)}; \tag{27a}$$

$$\tilde{\boldsymbol{v}}_0(t) - \underline{\mathrm{v}} \geq f^{-1}(1-\epsilon)\sqrt{\tilde{\boldsymbol{v}}_1^2(t) + \cdots + \tilde{\boldsymbol{v}}_N^2(t)}; \tag{27b}$$

$$\bar{\mathrm{I}} - \tilde{\boldsymbol{l}}_0(t) \geq f^{-1}(1-\epsilon)\sqrt{\tilde{\boldsymbol{l}}_1^2(t) + \cdots + \tilde{\boldsymbol{l}}_N^2(t)}. \tag{27c}$$

Indeed, it is seen that Eq. (24) are satisfied iff $\exists \gamma_l > 0$ and $\gamma_v > 0$ such that

$$\tilde{\boldsymbol{v}}_0(t) + f^{-1}(1-\epsilon)\gamma_v \leq \overline{\mathrm{v}} \tag{28a}$$

$$\tilde{\boldsymbol{v}}_0(t) - f^{-1}(1-\epsilon)\gamma_v \geq \underline{\mathrm{v}} \tag{28b}$$

$$\gamma_v \geq \sqrt{\tilde{\boldsymbol{v}}_1^2(t) + \cdots + \tilde{\boldsymbol{v}}_N^2(t)} \tag{28c}$$

$$\gamma_l \geq \sqrt{\tilde{\boldsymbol{l}}_1^2(t) + \cdots + \tilde{\boldsymbol{l}}_N^2(t)} \tag{28d}$$

$$\tilde{\boldsymbol{l}}_0(t) + f^{-1}(1-\epsilon)\gamma_l \leq \bar{\mathrm{I}}. \tag{28e}$$

where $\tilde{\boldsymbol{v}}_i(t)$ and $\tilde{\boldsymbol{l}}_i(t)$ is the gPC coefficient of the random $\boldsymbol{v}(\boldsymbol{\xi}, t)$ and $\boldsymbol{l}(\boldsymbol{\xi}, t)$ respectively.

C. Pseudospectral Model of Stochastic Economic Dispatch

Using the gPC spectral model to approximate the random variables, the expected value of random variable can be described by the first coefficient in its expression. Substituting the convex approximation of constraints (28) into the chance constraints (23) in the SNO problem (16)∼(23), the problem is redescribed as follows:

$$\mathbf{P}: \min_{\tilde{\boldsymbol{S}}(t), \boldsymbol{S}(\boldsymbol{\xi}, t), \boldsymbol{u}(t)} \quad \sum_{t \in \mathcal{T}} \tilde{f}_{l,t} \tag{29a}$$

$$\text{s.t.} \quad \forall t \in \mathcal{T}:$$

$$\mathrm{C}\boldsymbol{S}(\boldsymbol{\xi}, t) = \mathrm{b}_t + \boldsymbol{u}(t) + \mathrm{a}_t \boldsymbol{\xi}, \forall \boldsymbol{\xi} \in \Xi; \tag{29b}$$

$$\boldsymbol{g}(\boldsymbol{S}(\boldsymbol{\xi}, t)) \preceq \mathbf{0}, \quad \forall \boldsymbol{\xi} \in \Xi; \tag{29c}$$

$$\boldsymbol{\Phi}(\boldsymbol{\xi})\tilde{\boldsymbol{S}}(t) = \boldsymbol{S}(\boldsymbol{\xi}, t), \forall \boldsymbol{\xi} \in \Xi; \tag{29d}$$

$$(22), \quad (28). \tag{29e}$$

where the objective function $\tilde{f}_{l,t} = \sum_{j \in \Omega} \mathrm{R}_j \tilde{\boldsymbol{l}}_{j0}(t) + \boldsymbol{\rho}\boldsymbol{u}(t)$. $\boldsymbol{\Phi}(\boldsymbol{\xi}) = [\phi_0(\boldsymbol{\xi}), \phi_1(\boldsymbol{\xi}), \ldots, \phi_N(\boldsymbol{\xi})]$ is basis of gPC in terms of the distribution of input $\boldsymbol{\xi}$. The gPC coefficient $\tilde{\boldsymbol{S}}(t) = [\tilde{\boldsymbol{S}}_0(t), \tilde{\boldsymbol{S}}_1(t), \ldots, \tilde{\boldsymbol{S}}_N(t)]^T$ is the auxiliary variable in the problem.

Constraints (29b)–(29c) are the power balance constraints at the realizations of the random variable $\boldsymbol{\xi}$, where the inequality (29c) is the conic shown as (18). Constraints (29d) denote that the Nth-degree gPC approximation of the random state variables hold on every collocation points.

To solve $\mathbf{P}$ in (29), Monte Carlo is commonly used simple scheme however it is to be blamed for its low convergence rate and heavy computational cost when the system should be solved for every samples in the stochastic space Ξ. Stochastic collocation method is an alternative scheme that it need subspace of the stochastic space Ξ and has exponentially convergence, but it is recognized as a computational challenge to deal with high dimensional case.

Remark 3: To prevent the problem from becoming underdetermined, we require the number of collocation points not to be smaller than the number of gPC expansion terms. For the multivariate case, the basis is a tensor product of univariate polynomials (see (12)). By using the tensor product construction, the total number collocation points is m^d where m is the number of samples in each dimension. Obviously, in order to describe the input uncertainty, the size of samples increases exponentially with the dimension of the input uncertainty if you want to approximate gPC coefficients .

Remark 4: For the choice of the collocation points $\boldsymbol{\xi}^k := (\xi_1^k, \xi_2^k, \ldots, \xi_d^k)$, which is a vector of sampling points for the d random variables, it has become popular to use points which lie on a sparse grid in the stochastic space generated by Smolyak's algorithm [16]. While this approach performs well when o and d are small, it may become impractical for high-dimensional random inputs.

Due to the limited computational sources, it is significant in exploiting the approximate sparsity of the coefficient $\tilde{\boldsymbol{S}}(t)$ in high-dimensional cases. The techniques from the field of compressive sampling [39] can achieve an accurate reconstruction with a small number of samples. Moreover, a small portion of collocation points in $k \in \mathcal{K}$ is randomly selected as training sets to approximate coefficients, to enhance the efficiency of solving (29) in the following section.

IV. Compressive Sensing Based Optimization

In this section, sparse polynomial chaos approximation is proposed to quantify uncertainty in economic dispatch of DGs as the distribution system has high-dimensional stochastic inputs. To this end, we extend ideas from the field of compressive sampling.

A. Compressive Function Approximation

Suppose that $\{\boldsymbol{\xi}^k\}_{k=1}^K \subset \Xi$ is a finite sample set of realizations, typically chosen randomly from an appropriate distribution, let $\overline{\boldsymbol{\xi}} = (\boldsymbol{\xi}^1, \boldsymbol{\xi}^2, \ldots, \boldsymbol{\xi}^K)$ and consider the corresponding model outputs $\boldsymbol{S}(\overline{\boldsymbol{\xi}}, t) = [\boldsymbol{S}(\boldsymbol{\xi}^1, t), \ldots, \boldsymbol{S}(\boldsymbol{\xi}^K, t)]^T$. Specifically, we would like to approximate the coefficients $\tilde{\boldsymbol{S}}(t) = [\tilde{\boldsymbol{S}}_0(t), \tilde{\boldsymbol{S}}_1(t), \ldots, \tilde{\boldsymbol{S}}_N(t)]^T$, $K < N$, by solving the following optimization problem [40]:

$$\tilde{\boldsymbol{S}}^*(t) = \arg\min_{\tilde{\boldsymbol{S}}(t)} \left\{ \left\| \tilde{\boldsymbol{S}}(t) \right\|_0 \middle| \boldsymbol{\Psi} \tilde{\boldsymbol{S}}(t) = \boldsymbol{S}\left(\overline{\boldsymbol{\xi}}, t\right) \right\} \tag{30}$$

where the semi-norm $\|\tilde{\boldsymbol{S}}(t)\|_0$ is the number of non-zero components of $\tilde{\boldsymbol{S}}(t)$. The measurement matrix $\boldsymbol{\Psi}$ is generated by setting $\Psi_{ij} = \phi_i(\boldsymbol{\xi}^j)$.

In general, the global minimum solution of (30) is not unique and is NP-hard to compute. Further developments in compressive sampling resulted in a convex relaxation of problem (30) by minimization of the l_1-norm instead. Columns of $\boldsymbol{\Psi}$ with large anticipated coefficients should not be heavily penalized when used in the approximation. Accordingly, it is reasonable to use this a priori information to improve the accuracy of sparse approximations. In this work, we explore the use of a priori knowledge of the gPC coefficients as a weighted l_1-minimization:

$$\tilde{\boldsymbol{S}}_W^*(t) = \arg\min_{\tilde{\boldsymbol{S}}(t)} \left\{ \left\| \boldsymbol{W} \tilde{\boldsymbol{S}}(t) \right\|_1 \mid \boldsymbol{\Psi} \tilde{\boldsymbol{S}}(t) = \boldsymbol{S}(\overline{\boldsymbol{\xi}}, t) \right\} \tag{31}$$

where the matrix $\boldsymbol{W}$ is a diagonal positive-definite matrix. A natural choice for the (i, i) entry in this matrix for this case is $W_{ii} = \|\boldsymbol{\Psi}_i\|_2$.

Note that, the purpose of weighting the l_1 cost function with $\boldsymbol{W}$ is to prevent the optimization from biasing toward the non-zero entries in $\tilde{\boldsymbol{S}}(t)$ whose corresponding columns in $\boldsymbol{\Psi}$ have large norms. Further more, the optimal solution $\tilde{\boldsymbol{S}}_W^*(t)$ in (30) can be obtained by solving the following unconstraint problem:

$$\tilde{\boldsymbol{S}}_\lambda^\star(t) = \arg\min_{\tilde{\boldsymbol{S}}(t)} \left\{ \left\| \boldsymbol{W} \tilde{\boldsymbol{S}}(t) \right\|_1 + \frac{1}{2\lambda_S} \left\| \boldsymbol{\Psi} \tilde{\boldsymbol{S}}(t) - \boldsymbol{S}\left(\overline{\boldsymbol{\xi}}, t\right) \right\|_2^2 \right\} \tag{32}$$

where $\lambda_S \geq 0$ is interpreted as a relative weight or trade-off parameter between the two terms. Moreover, for $\lambda_S > \|\boldsymbol{\Psi}^T \boldsymbol{S}(\overline{\boldsymbol{\xi}}, t)\|_\infty$, $\tilde{\boldsymbol{S}}_\lambda^\star(t) \approx 0$, and for $\lambda_S \to 0$, $\tilde{\boldsymbol{S}}_\lambda^\star(t)$ converges to the optimum solution $\tilde{\boldsymbol{S}}^*(t)$ in (30).

Remark 5: In order to approximate $\boldsymbol{S}(\boldsymbol{\xi}, t)$, it suffices to approximate its coefficients $\tilde{\boldsymbol{S}}(t)$ from the measurements of model outputs $\boldsymbol{S}(\overline{\boldsymbol{\xi}}, t)$. There are two main goals should be considered: 1) the estimation $\boldsymbol{\Psi}\tilde{\boldsymbol{S}}(t)$ to be close to $\boldsymbol{S}(\boldsymbol{\xi}, t)$; 2) it should involve as few columns from $\boldsymbol{\Psi}$ as possible.

B. Distributed Implementation

Based on a small number of samples, the technique of compressive seeks a sparse approximation of the gPC to reconstruct solution in the random space. Thus, to exploit approximate sparsity of the coefficients $\tilde{S}(t)$ in high-dimensional cases, the l_1 norm of coefficients should also be considered in the minimization. Mathematically speaking, our goals are to minimize both $\|\|_1$ and cost function of economic dispatch in (**P**). Accordingly, we transform this multi-objective optimization problem into a regularized problem by solving problem:

$$\begin{aligned}
\mathbf{P1}: \quad & \min_{\boldsymbol{S}(\overline{\boldsymbol{\xi}}, t), \tilde{\boldsymbol{S}}(t), \boldsymbol{u}(t)} \sum_{t \in \mathcal{T}} \left(\tilde{f}_{l,t} + \left\| \boldsymbol{W} \tilde{\boldsymbol{S}}(t) \right\|_1 \right) && \text{(33a)} \\
& \text{s.t.} \quad \forall t \in \mathcal{T}: \\
& \mathrm{C}\boldsymbol{S}\left(\overline{\boldsymbol{\xi}}, t\right) = \mathrm{b}_t + \boldsymbol{u}(t) + \mathrm{a}_t \overline{\boldsymbol{\xi}}; && \text{(33b)} \\
& \boldsymbol{g}\left(\boldsymbol{S}\left(\overline{\boldsymbol{\xi}}, t\right)\right) \preceq \mathbf{0}; && \text{(33c)} \\
& \boldsymbol{\Psi} \tilde{\boldsymbol{S}}(t) = \boldsymbol{S}\left(\overline{\boldsymbol{\xi}}, t\right); && \text{(33d)} \\
& (22), \quad (28). && \text{(33e)}
\end{aligned}$$

The methods discussed above are a good way to accomplish the stochastic economic dispatch, and it can get a reliable solution to **P1** in (33) with little programming effort. However, for large-scale applications, general purpose optimizers seem slow and can perhaps be improved by special purpose techniques. We define two subproblems: one (**P2**) in the economical dispatching variables $\{\boldsymbol{S}(\overline{\boldsymbol{\xi}}, t), \boldsymbol{u}(t)\}_{t \in \mathcal{T}}$ and one (**P3**) in UQ variables $\{\tilde{\boldsymbol{S}}(t)\}_{t \in \mathcal{T}}$.

It is observed that the problem **P1** is able to decomposed into **P2** and **P3** except for the coupled linear equality constraints (33d). Forming the augmented Lagrangian corresponding to the constraints (33d) (with the Lagrange multiplier $\boldsymbol{\mu}$) and combining the linear and quadratic terms in the augmented Lagrangian,

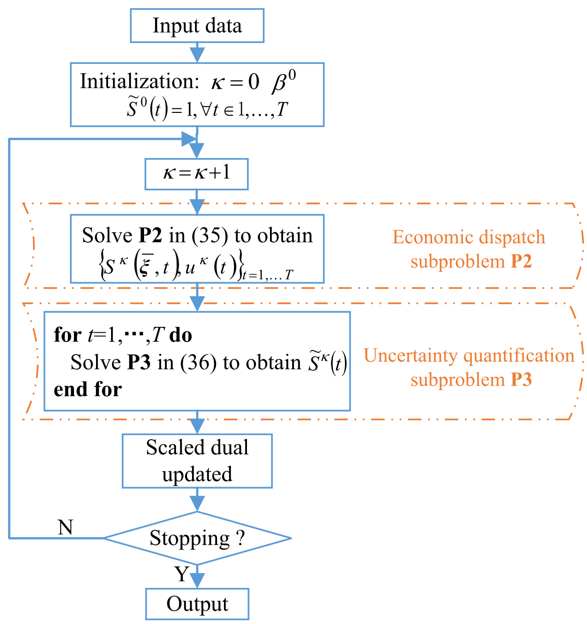

Fig. 1. The flowchart of the proposed algorithm.

that is

$$L_0\left(\boldsymbol{S}\left(\bar{\boldsymbol{\xi}},t\right),\tilde{\boldsymbol{S}}(t),\boldsymbol{u}(t),\boldsymbol{\mu}\right)=\sum_{t\in\mathcal{T}}\left(\tilde{f}_{l,t}+\left\|\boldsymbol{W}\tilde{\boldsymbol{S}}(t)\right\|_1\right.$$
$$\left.+\frac{1}{2\lambda}\left\|\boldsymbol{\Psi}\tilde{\boldsymbol{S}}(t)-\boldsymbol{S}\left(\bar{\boldsymbol{\xi}},t\right)+\boldsymbol{\beta}\right\|_2^2+\frac{1}{2\lambda}\|\boldsymbol{\beta}\|_2^2\right) \tag{34}$$

where $\boldsymbol{\beta}=\lambda\boldsymbol{\mu}$ is the scaled dual variable, $\lambda>0$ is a parameter. Thus the distributed optimization algorithm based on the scaled ADMM is proposed.

As the flowchart of proposed algorithm shown in Fig. 1, the input data including the randomly selected samples of random variables $\boldsymbol{\xi}$ in their space Ξ, gPC basis associated with $\boldsymbol{\xi}$, and system parameters (e.g., impedance, topology of electric network). What is more, the distributed algorithm consists of the following steps:

Step 1: Generate input samples $\bar{\boldsymbol{\xi}}=(\boldsymbol{\xi}^1,\boldsymbol{\xi}^2,\ldots,\boldsymbol{\xi}^K)^T$ based on the distribution of $\boldsymbol{\xi}$.

Step 2: Select gPC basis functions $\{\boldsymbol{\Phi}_n\}_{n=1}^N$ associated with $\boldsymbol{\xi}$ and then generate the measurement matrix $\boldsymbol{\Psi}$ by setting $\Psi_{ij}=\boldsymbol{\Phi}_i(\boldsymbol{\xi}^j)$. And generate the weighted matrix $\boldsymbol{W}$ by setting $W_{ii}=\|\boldsymbol{\Psi_i}\|_2$.

Step 3: Initialize $\kappa=0$, set the initial solution $\boldsymbol{\beta}^0$ and $\tilde{\boldsymbol{S}}^0(t)=\mathbf{1},\forall t\in\mathcal{T}$.

Step 4: Increment κ by 1 and perform the following steps:

1) Receive $\{\tilde{\boldsymbol{S}}^{\kappa-1}(t)\}_{t\in\mathcal{T}}$ from the problem **P3** at the last iteration. Update $\{\boldsymbol{S}^{\kappa}(\bar{\boldsymbol{\xi}},t),\boldsymbol{u}^{\kappa}(t)\}_{t\in\mathcal{T}}$ by solving the optimization problem **P2** in (35).

$$\min_{\boldsymbol{S}(\bar{\boldsymbol{\xi}},t),\boldsymbol{u}(t)}\sum_{t\in\mathcal{T}}\left(\tilde{f}_{l,t}+\frac{1}{2\lambda}\left\|\boldsymbol{\Psi}\tilde{\boldsymbol{S}}^{\kappa-1}(t)\right.\right.$$
$$\left.\left.-\boldsymbol{S}\left(\bar{\boldsymbol{\xi}},t\right)-\boldsymbol{\beta}^{\kappa-1}\right\|_2^2\right)$$
$$\text{s.t.}\quad \forall t\in\mathcal{T}:\ (22),(33b),(33c). \tag{35}$$

2) Receive $\{\boldsymbol{S}^{\kappa}(\bar{\boldsymbol{\xi}},t),\boldsymbol{u}^{\kappa}(t)\}_{t\in\mathcal{T}}$ from the problem **P2**. Update $\tilde{\boldsymbol{S}}^{\kappa}(t)$ by solving the optimization problem **P3** in (36) for all $t\in\mathcal{T}$:

$$\min_{\tilde{\boldsymbol{S}}(t)}\ \left\|\boldsymbol{W}\tilde{\boldsymbol{S}}(t)\right\|_1+\frac{1}{2\lambda}\left\|\boldsymbol{\Psi}\tilde{\boldsymbol{S}}(t)-\boldsymbol{S}^{\kappa}\left(\bar{\boldsymbol{\xi}},t\right)-\boldsymbol{\beta}^{\kappa-1}\right\|_2^2$$
$$\text{s.t.}\quad (28). \tag{36}$$

3) Scaled dual variable update:

$$\boldsymbol{\beta}^{\kappa}=\boldsymbol{\beta}^{\kappa-1}+\boldsymbol{\Psi}\tilde{\boldsymbol{S}}^{\kappa}(t)-\boldsymbol{S}^{\kappa}\left(\bar{\boldsymbol{\xi}},t\right) \tag{37}$$

4) Stopping rule: Compute the residual errors

$$\Delta_1=\max_{t\in\mathcal{T}}\left\|\boldsymbol{u}^{\kappa}(t)-\boldsymbol{u}^{\kappa-1}(t)\right\|_\infty$$
$$\Delta_2=\max_{t\in\mathcal{T}}\left\|\boldsymbol{\Psi}\tilde{\boldsymbol{S}}^{\kappa}(t)-\boldsymbol{S}^{\kappa}\left(\bar{\boldsymbol{\xi}},t\right)\right\|_\infty \tag{38}$$

If the errors are smaller than some predetermined threshold, stop. Otherwise, apply another iteration.

Step 5: Output the optimal economic dispatched power of DGs $\boldsymbol{u}^\star(t)=\boldsymbol{u}^{\kappa}(t)$ over time t, meanwhile, set $\tilde{\boldsymbol{S}}^\star(t)=\tilde{\boldsymbol{S}}^{\kappa}(t)$ and construct gPC expansion $\boldsymbol{S}(\boldsymbol{\xi},t)\approx\boldsymbol{\Phi}(\boldsymbol{\xi})\tilde{\boldsymbol{S}}^\star(t)$ to accomplish the uncertainty quantification of the state variable, such as voltage and current, in the distribution system with DGs.

Remark 6: Note that, in above proposed algorithm, the separate sub-problems P2 and P3 are solved in parallel. Since all the feasible sets of these optimization problems are convex, it guarantee the convergence of the proposed distributed algorithm [41], [42].

C. Stability of the Sparsest Compressive Sensing Solution

The ability of weighted l_1-minimization to accurately determine the large coefficients of the gPC is determined by the properties of the matrix $\boldsymbol{\Psi}$ and the sparsity of aPC representation of the stochastic state output $\boldsymbol{S}(\boldsymbol{\xi},t)$.

Comparing the optimal solution $\tilde{\boldsymbol{S}}^\star_\lambda(t)$ in (32) with a solution $\tilde{\boldsymbol{S}}^\sharp(t):=(\tilde{\boldsymbol{S}}^\sharp_0(t),\tilde{\boldsymbol{S}}^\sharp_1(t),\ldots,\tilde{\boldsymbol{S}}^\sharp_N(t))$, which is the vector of gPC coefficient calculated by above Galerkin projection (14), the truncation error $\|\tilde{\boldsymbol{S}}^\star_\lambda(t)-\tilde{\boldsymbol{S}}^\sharp(t)\|_2$ incurred from the sparse approximation. The small level of truncation error implies that the exact reconstructions are themselves approximated by a sparse solution.

Definition 1: (Mutual Coherence [18]) The mutual coherence is a tractable property of the measurement matrix $\boldsymbol{\Psi}\in\mathbb{R}^{K\times N}$ for calculation, it is given by:

$$\mu(\boldsymbol{\Psi})=\max_{1\le i,j\le N,i\ne j}\frac{|\boldsymbol{\Psi}_i^T\boldsymbol{\Psi}_j|}{\|\boldsymbol{\Psi}_i\|_2\|\boldsymbol{\Psi}_j\|_2} \tag{39}$$

where $\boldsymbol{\Psi}_i$, $\boldsymbol{\Psi}_j$ are corresponding column of $\boldsymbol{\Psi}$.

The mutual coherence is an indicator of dependence between columns of the matrix $\boldsymbol{\Psi}$. In general, small $\mu(\boldsymbol{\Psi})$ yields better ability to recover a sparse solution with the compressive sensing method.

Theorem 1: Let $\boldsymbol{S}^0(\boldsymbol{\xi},t)=\boldsymbol{\Psi}\tilde{\boldsymbol{S}}^0(t)$ be the sparse gPC approximation of $\boldsymbol{S}(\boldsymbol{\xi},t)$ in problem **P** (29), it satisfies

$$\left\|\tilde{\boldsymbol{S}}^0(t)\right\|_0<(1+1/\mu(\boldsymbol{\Psi}))/4 \tag{40}$$

and

$$\|\boldsymbol{S}^0(\boldsymbol{\xi}, t) - \boldsymbol{S}(\boldsymbol{\xi}, t)\|_2 \leq \delta \tag{41}$$

where δ is the error tolerance of the sparse representation. The iterative solution $\tilde{\boldsymbol{S}}^\kappa(t)$ in **P1** (33) obtained by the distributed algorithm proposed in IV-B satisfies $\|\tilde{\boldsymbol{S}}^\kappa(t) - \tilde{\boldsymbol{S}}^\star(t)\|_2 \leq c_1$, then it must obey

$$\left\|\tilde{\boldsymbol{S}}^\kappa(t) - \tilde{\boldsymbol{S}}^0(t)\right\|_2 \leq c_1 + c_2 \tag{42}$$

where $c_2 = \frac{4\delta^2}{1-\mu(\boldsymbol{\Psi})(4\|\tilde{\boldsymbol{S}}^0(t)\|_0-1)}$ and $\tilde{\boldsymbol{S}}^\star(t)$ is the optimal solution of (33) calculated by centralized algorithm.

Proof: The left part of Eq. (42) equal to

$$\begin{aligned}\left\|\tilde{\boldsymbol{S}}^\kappa(t) - \tilde{\boldsymbol{S}}^0(t)\right\|_2 &= \left\|\tilde{\boldsymbol{S}}^\kappa(t) - \tilde{\boldsymbol{S}}^\star(t) + \tilde{\boldsymbol{S}}^\star(t) - \tilde{\boldsymbol{S}}^0(t)\right\|_2 \\ &\leq \left\|\tilde{\boldsymbol{S}}^\kappa(t) - \tilde{\boldsymbol{S}}^\star(t)\right\|_2 + \left\|\tilde{\boldsymbol{S}}^\star(t) - \tilde{\boldsymbol{S}}^0(t)\right\|_2\end{aligned}$$

where the above inequality is in terms of the triangle inequality of the vector norm. According to the Stability Theorem 8 in [43], if the assumed condition is satisfied, the weighted l_1 minimization solution $\tilde{\boldsymbol{S}}^\star(t)$ must obey

$$\left\|\tilde{\boldsymbol{S}}^\star(t) - \tilde{\boldsymbol{S}}^0(t)\right\|_2 \leq \frac{4\delta^2}{1-\mu(\boldsymbol{\Psi})\left(4\left\|\tilde{\boldsymbol{S}}^0(t)\right\|_0 - 1\right)}$$

And the distributed solution $\tilde{\boldsymbol{S}}^\kappa(t)$ is convergent to the centralized solution $\tilde{\boldsymbol{S}}^\star(t)$ with the error tolerance c_2. So this concludes the proof.

The compressive sensing based strategy enables an accurate recovery of the solution to stochastic optimization problem with high-dimensional random inputs. In the pseudospectral model of stochastic economic dispatch (see (29)), the gPC is introduced to approximately represent the random state variables of power system. By exploiting the approximate sparsity of the gPC coefficients, we seek to achieve an accurate reconstruction with a number of random solution samples that is significantly smaller than the cardinality of the gPC basis. Theorem 1 discusses the quality of the solution identified from the proposed algorithm. And the stability means that the gPC coefficients recovered from the weighted l_1 minimization do not blow up in the presence of the truncation error.

V. Numerical Tests

A. System Setup

The distribution system considered for the test is the modified 33-buses benchmark examples. As shown in Fig. 2(a), it is a 12.66 kV distribution system with a peak load of 5084.26 + j2547.32 kVA. Moreover, the data of the system are given in [27]. The optimization horizon, $\mathcal{T} = \{1, 2, \ldots, 24\}$, is taken to be a day, and we discretize the day into 24 uniform time intervals, each of which is equal to 1 hour. There are two kinds of DGs such as photovoltaic system and wind turbine considered in our study. It is assumed that the solar-based DGs are placed at node 4, 7, 8, 24, 25, and wind-based DGs are placed at node 14, 16, 20, 30, 32.

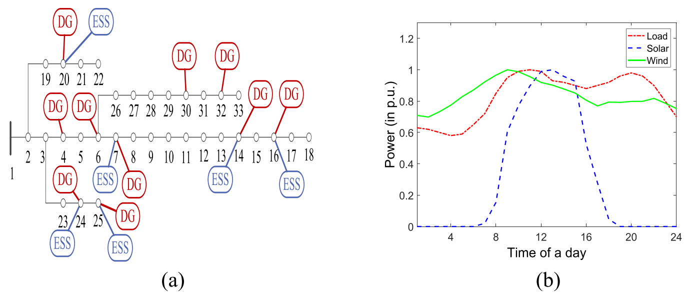

Fig. 2. (a) The modified 33-buses distribution system with DGs and ESSs. (b) Hourly average load and power generated by solar/wind based-DG of a day.

The forecast errors are modeled as zero mean Gaussian random variables with a standard deviation corresponding to 10% of the forecasted production. It is assumed that the renewable based distributed generator is operating withe a constant power factor 0.95 capacitive. The acceptable violation probability is set to $\epsilon = 5\%$.

And the cost of the battery is \$30/kWh. The battery storage system are injected at the node 7, 14, 15, 20, 24 and 25. The power of battery is designed to be dispatched economically to maintain the minimum active power loss in the distribution system, where the optimization model is described in Eq. (29). Here, the 3rd-order generalized Polynomial-chaos (gPC) expansion for the corresponding random state variables in the distribution system is utilized.

B. The Model of Uncertainty

In order to assess the feasibility of the KLE approach for representing forecast error, the chronological weather data of the Zhoushan islands in China over about the four years period is selected [44]. These data are recorded by a cup generator anemometer, radiation sensor and thermometer at a height of 50m. And the weather forecast model [28] is employed to provide day-ahead prediction of wind power and solar power in a specific region. The resulting hourly-average renewable power of a day is shown in Fig. 2(b).

The hourly error between the daily power samples and the predicted hourly-average power can be constructed to be independent samples from a 24-dimensional random field. Given a set of discrete realizations of a 24-dimensional field $\{[err(\xi^k, 1), \ldots, err(\xi^k, 24)]\}_k$, the 24×24 covariance matrix can be estimated from these realizations [30]. Thus, the eigenvalues μ_i and eigenvectors $f_i(t)$ in KLE (as shown in Eq. (43)) is obtained via the principal component analysis of the covariance matrix.

$$err(\xi, t) = \sum_{i=1}^{24} \sqrt{\mu_i} f_i(t) \xi_i \tag{43}$$

Define $\sigma_v(M)$ as the percentages of the total variance explained by truncated M-th order KLE.

$$\sigma_v(M) = \frac{\int_{\mathcal{T}} \text{var}\left[err^M(\xi, t)\right] dt}{\int_{\mathcal{T}} \text{var}\left[err(\xi, t)\right] dt} = \frac{\sum_{i=1}^{M} \mu_i}{\sum_{i=1}^{24} \mu_i} \tag{44}$$

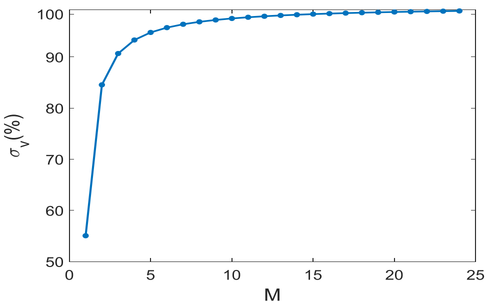

Fig. 3. Percentage of the total variance as increasing number of KLE terms.

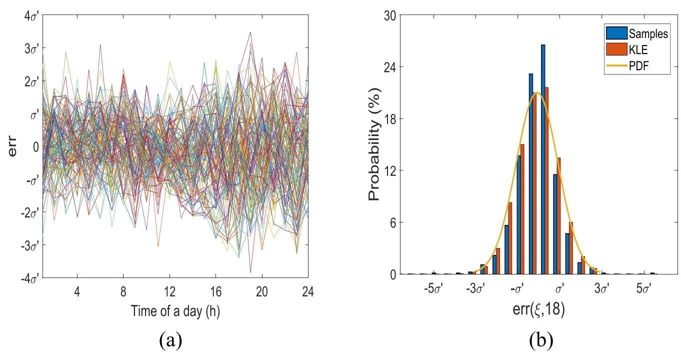

Fig. 4. (a) The samples of the stochastic forecast error. (b) Histograms of the forecast error samples (depicted in blue) and distribution of error at time $t = 18$ (depicted in red). The PDF for a Gaussian distribution is shown in orange line.

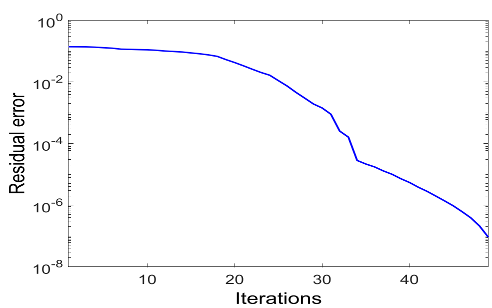

Fig. 5. Convergence of the distributed optimization algorithm for stochastic economic dispatch.

In Fig. 3, we illustrate the influence of the order terms on the fractional variance given in Eq. (44). It can be seen that $M = 5$ are sufficient to capture approximately 95% of the total variance.

The truncated KLE $err^M(\xi, t)$ with $M = 5$ terms is utilized to model the input random process of the forecast error. Fig. 4(a) shows the samples of the stochastic forecast error and an examination of the sample histograms provided in Fig. 4(b). As can be seen in Fig. 4 that the Gaussian distribution can approximately fit the forecast error distributions for the wind plants, and the synthesized samples of fifth-order truncated KLE approximation can match the target well.

C. Results of the Stochastic Economic Dispatch

1) Convergence of the Distributed Implementation: Fig. 5 shows the convergence of distributed stochastic optimization using the algorithm described in Section IV-B. As can be seen

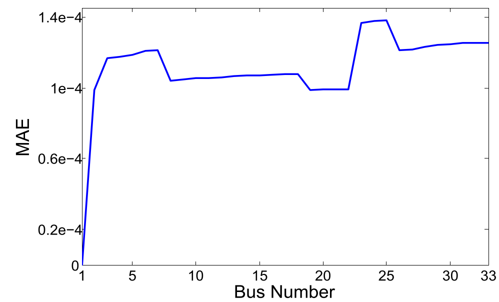

Fig. 6. The mean absolute error of the bus voltage.

from the relative residual error versus the number of iterations in Fig. 5, the distributed optimization algorithm requires dozens of iterations to achieve any relative error bellow 10-5. It can be concluded that the proposed distributed algorithm is convergent and efficient.

2) Feasibility of Conic Relaxation in Power Flow: By using the proposed compressive sensing-based distributed algorithm (CS-algorithm), we obtain the optimal solution $(\boldsymbol{v}^\star(\boldsymbol{\xi}, t), u^\star(t), t = 1, \ldots, T)$. To investigate the exactness of the conic relaxation of power flow in proposed strategy, let the controllable injected power be $u^\star(t)$ then the non-linear power flow equations are calculated by using the traditional Newton-Raphson iteration. Hence, we describe the difference in the value of calculated bus voltage between the optimal solution $\boldsymbol{v}^\star(\boldsymbol{\xi}, t)$ and Newton-Raphson method $\boldsymbol{v}'(\boldsymbol{\xi}, t)$, so as to verify the accuracy of the conic relaxation.

Define the mean absolute error (MAE) of the bus voltage magnitude as

$$MAE_j = \max_{t \in \mathcal{T}} \frac{1}{K} \sum_{k=1}^{K} \left| v_j^\star(\boldsymbol{\xi}^k, t) - v_j'(\boldsymbol{\xi}^k, t) \right| \quad (45)$$

The deviations of voltage magnitude at all buses between the CS-algorithm solution and the Newton-Raphson solution are illustrated in Fig. 6. The maximum mean absolute error of the bus voltage magnitude is about 10^{-4} which is almost negligibly small for practical purposes.

3) Effect of Stochastic Optimization: Based on the pseudospectral model of stochastic economic dispatch developed in this paper, two other approaches are introduced to compare the accuracy of the proposed CS-algorithm: (C1) The stochastic collocation method: solve the problem $\mathbf{P}$ in Eq. (29) with 5000 collocation points in the random space generated by Smolyak's algorithm. (C2) The Monte Carlo (MC) simulation: solve the economic dispatch problem $\mathbf{P}$ in Eq. (29) via 10^7 random samples of the forecast uncertainty drawn from a multivariate Gaussian distribution.

As shown in Table I, it summarizes the test results. The stochastic collocation method obtain the nearly optimal solution, it indicates the rationality of the pseudospectral model of the optimization problem. The operation cost and average active power losses of the proposed economic dispatch strategy CS-algorithm are 1.8275 MWh and \$12524.83 respectively, which are similar to the results of MC simulation methods. According

TABLE I
COMPARISON OF DIFFERENT APPROACHES OF SOLVING THE STOCHASTIC ECONOMIC DISPATCH

Method	Losses (MWh)	Cost ($)	time (s)	sample size	ϵ_J (%)
CS-algorithm	1.8275	12524.83	11.8	200	5.1
C1	1.8273	12477.5	167	5000	4.9
C2	1.8273	12458.31	5879	10^7	5

TABLE II
MAXIMUM OBSERVED VIOLATION PROBABILITY ϵ_J AND OPERATION COST FOR DIFFERENT SETTINGS OF VIOLATION PROBABILITY ϵ

ϵ (%)	Cost ($)	ϵ_J(%)
1	12900.2	1.4
5	12524.83	5.1
10	11987.71	9.6
15	11021.54	14.7

to the size of required samples, the proposed CS-algorithm has more advantages since it only needs 200 samples to accomplish the stochastic economic dispatch and reach required accuracy. The maximum observed probability (ϵ_J) of constraint violation for three different method is listed in the sixth column of Table I.

Additionally, to check whether the assumption of a Gaussian distribution leads to accurate results, we perform the sample test via Monte Carlo simulation with 10^7 samples after solving the problem. The sample test is performed to analyze the constraint violations for voltage limit and current limit. For different settings of violation probability in chance constraints, the cost of economic dispatch and results of sample test are listed in Table II. The operation cost decrease as the violation probability ϵ is increased from 1% to 10%. The probability of meeting voltage and current constraint is not expected to strictly hold. There is inaccuracies due to non-normally distributed samples, the difference is however not particularly large, and the solution of the proposed method is conservative when the value of ϵ is large. Although the actual current and voltage magnitude are not normally distributed, the Gaussian assumption appears to be reasonable in our studies.

The ESS devices are located at the same bus as DGs and is able to directly manage the fluctuated renewable energy. The operating schedule for the ESS devices on different buses are shown in Fig. 7. It can be seen from the figure that the ESS devices can absorb the surplus energy when the power generated by DGs reached peak level at midday. However, during the periods when there is less renewable power, the ESS devices generate power.

In addition to the optimal result of this chance constrained stochastic OPF, we can obtain the gPC of the uncertain voltage and current directly, thus the average and variance of the random variable can be computed by the coefficients of gPC. As can be see in Fig. 8, the error bar represent the fluctuation range of bus voltage at time $t = 9$. The proposed algorithm drives the voltage magnitudes within the desired range in spite of forecasting error.

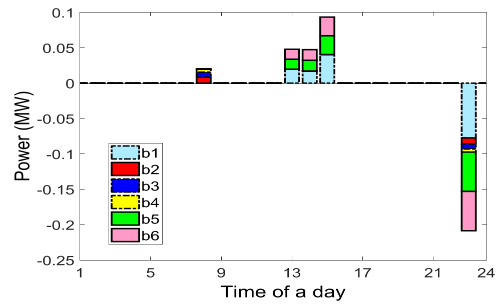

Fig. 7. The hourly output power of ESS on corresponding buses.

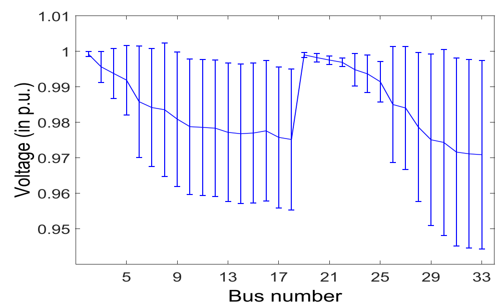

Fig. 8. The error bar of bus voltage at time $t = 9$.

TABLE III
MOMENTS OF THE 33-BUS EXAMPLE

Performance	$v_{13}(\boldsymbol{\xi}, t)$ (p.u.) CS-algorithm	MC	$f_l(\boldsymbol{\xi}, t)$ (MWh) CS-algorithm	MC
mean	0.9767	0.9766	0.0643	0.0645
var.	0.0121	0.0123	0.0177	0.018

D. Performance of Associated UQ

Take one bus voltage and system power loss as example, we use the following results to display the performance of compressive sensing based uncertainty quantification.

In order to check the accuracy, Table III compares the mean values and standard deviations from the MC and compressive sensing algorithm, where the voltage of bus 13 and active power losses of the distribution system at time $t = 9$ are taken for example to be certified. The results are very close.

We display the approximate upper bound on coefficients of 3-rd order gPC obtained from the proposed algorithm in Fig. 9, where the blue squares represent the reference and the red asterisks circles the non-zero coefficients of the proposed algorithm. The reference is the gPC coefficient obtained using a sparse grid, with resulted in an approximation error below 10^{-8}.

To measure the performance of an approximation, we will use the Root-Mean-Square Error (RMSE). Specifically given a set of samples $\Xi_{test} = \{\boldsymbol{\xi}^k\}_{k=1}^{K'}$ and the corresponding samples of the true state variables, such as the bus13 voltage $v_{13}(\boldsymbol{\xi}^k, t)$, and the gPC approximation $v_{13}^N(\boldsymbol{\xi}^k, t)$, we compute

$$RMSE_t = \sqrt{\frac{1}{K'} \sum_{k=1}^{K'} \left| v_{13}^N(\boldsymbol{\xi}^k, t) - v_{13}(\boldsymbol{\xi}^k, t) \right|^2}$$

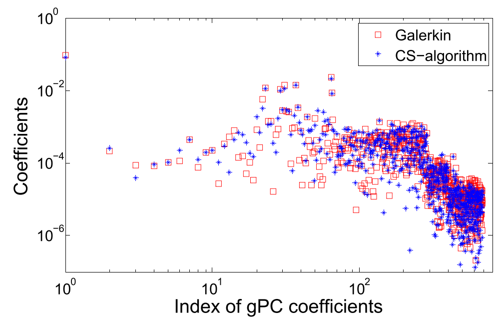

Fig. 9. Approximate gPC coefficients obtained by proposed algorithm vs. the reference coefficients.

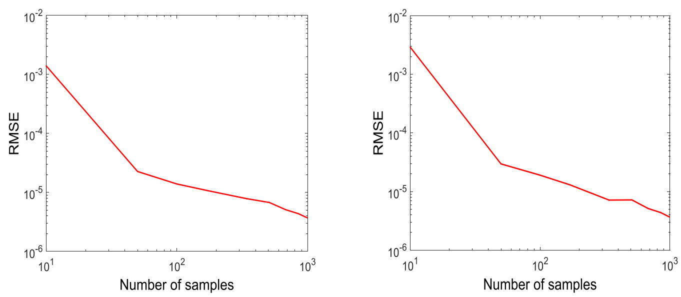

(a) (b)

Fig. 10. Convergence of the RMSE, with respect to increasing sample size, in the 3-rd order gPC approximation of (a) the bus13 voltage and (b) the system power loss.

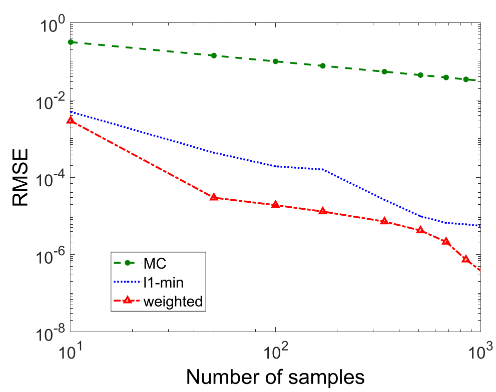

Fig. 11. Comparison of RMSE in the 3-rd order gPC approximation of power loss computed via Monte Carlo, l_1-minimization and the proposed weighted compressive sensing.

As shown in Fig. 10, it plots the RMSE $:= \max_{t\in\mathcal{T}} RMSE_t$ in the polynomial approximations for increasing number of samples. Fig. 10(a) and (b) plots the approximation error for 3-rd order gPC approximation of the bus13 voltage and system power loss respectively. With increasing sample number, the RMSE decrease sharply. Therefore, it is a feasible way choice to accomplish the stochastic dispatching of the 69-buses example by using 100 samples of 10 random variables.

Fig. 11 displays a comparison between the accuracy of l_1-minimization (l_1-min), weighted l_1-minimization and Monte Carlo(MC). With subset of realizations of uncertain variables, it is observed that both l_1-minimization (l_1-min) and weighted l_1-minimization algorithm result in smaller RMSE, compared to the MC. Additionally, for small sample size, the proposed weighted l_1-minimization outperforms the l_1-minimization. This is expected as the prior knowledge on the decay of coefficient has comparable effect on the accuracy as the solution realizations do.

VI. Conclusion

This paper has proposed a stochastic economic dispatch algorithm based on the sparse polynomial approximation and compressive sensing method. The economic dispatch problem is modeled by the chance-constrained stochastic programming formulation that it minimize the cost subject to power flow constraints, chance constraints and so on. The stochastic solutions are represented by the sparse polynomial chaos expansions obtained via weighted l_1 minimization. Although polynomial coefficients are considered additionally as auxiliary variables in the optimization problem, the chance constraints can be restated by the conic constraints of coefficients. To approximate the stochastic solution, there are lots of basis functions and simulation samples for problem with high-dimensional uncertainty. However, the proposed compressive sensing based algorithm can get the deterministic equivalents of the stochastic programming problem based on compressive samplings. The number of samples we need to calculate the optimal solution can be less than the number of basis functions. That is, the weighted l_1 minimization techniques is employed to break the curse of dimensionality, since multivariate functions posses expansions in orthogonal polynomial bases are approximately sparse. Finally, a distributed strategy is developed by using the alternating direction method of multipliers (ADMM), to enable economic dispatch and compressive sensing based uncertainty quantification pursue specific performance objectives.

Future work will investigate whether the compressive sensing based algorithm can benefit from the economic dispatch of renewable power with non-stationary non-gaussian stochastic process of forecast error. Moreover, we would like to investigate how the algorithm can be extended to solve the problem with original non-approximated AC power flow.

References

[1] C. Safta, R. L. Y. Chen, H. N. Najm, A. Pinar, and J. P. Watson, "Efficient uncertainty quantification in stochastic economic dispatch," *IEEE Trans. Power Syst.*, vol. 32, no. 4, pp. 2535–2546, Jul. 2017.

[2] H. Ming, L. Xie, M. Campi, S. Garatti, and P. R. Kumar, "Scenario-based economic dispatch with uncertain demand response," *IEEE Trans. Smart Grid*, Nov. 29, 2017.

[3] H. Zhang and P. Li, "Chance constrained programming for optimal power flow under uncertainty," *IEEE Trans. Power Syst.*, vol. 26, no. 4, pp. 2417–2424, Nov. 2011.

[4] T. Summers, J. Warrington, M. Morari, and J. Lygeros, "Stochastic optimal power flow based on convex approximations of chance constraints," in *Proc. Power Syst. Comput. Conf.*, Aug. 2014, pp. 1–7.

[5] R. A. Jabr, S. Karaki, and J. A. Korbane, "Robust multi-period OPF with storage and renewables," *IEEE Trans. Power Syst.*, vol. 30, no. 5, pp. 2790–2799, Sep. 2015.

[6] A. Venzke, L. Halilbasic, U. Markovic, G. Hug, and S. Chatzivasileiadis, "Convex relaxations of chance constrained ac optimal power flow," *IEEE Trans. Power Syst.*, vol. 33, no. 3, pp. 2829–2841, May 2018.

[7] L. Roald and G. Andersson, "Chance-constrained ac optimal power flow: Reformulations and efficient algorithms," *IEEE Trans. Power Syst.*, vol. 33, no. 3, pp. 2906–2918, May 2018.

[8] C. Duan, W. Fang, L. Jiang, L. Yao, and J. Liu, "Distributionally robust chance-constrained approximate AC-OPF with Wasserstein metric," *IEEE Trans. Power Syst.*, vol. 33, no. 5, pp. 4924–4936, Sep. 2018.
[9] G. Lin, M. Elizondo, S. Lu, and X. Wan, "Uncertainty quantification in dynamic simulations of large-scale power system models using the high-order probabilistic collocation method on sparse grids," *Int. J. Uncertainty Quantification*, vol. 4, no. 3, pp. 185–204, 2014.
[10] J. D. Jakeman and S. G. Roberts, "Local and dimension adaptive stochastic collocation for uncertainty quantification," in *Proc. Sparse Grids Appl.* Springer, 2012, pp. 181–203.
[11] D. Xiu and G. E. Karniadakis, "The Wiener–Askey polynomial chaos for stochastic differential equations," *SIAM J. Sci. Comput.*, vol. 24, no. 2, pp. 619–644, 2002.
[12] Z. Zhang, T. A. El-Moselhy, I. M. Elfadel, and L. Daniel, "Stochastic testing method for transistor-level uncertainty quantification based on generalized polynomial chaos," *IEEE Trans. Comput.-Aided Des. Integr. Circuits Syst.*, vol. 32, no. 10, pp. 1533–1545, Oct. 2013.
[13] H. N. Najm, "Uncertainty quantification and polynomial chaos techniques in computational fluid dynamics," *Annu. Rev. Fluid Mech.*, vol. 41, pp. 35–52, 2009.
[14] T. Mhlpfordt, T. Faulwasser, and V. Hagenmeyer, "Solving stochastic ac power flow via polynomial chaos expansion," in *Proc. IEEE Conf. Control Appl.*, Sep. 2016, pp. 70–76.
[15] T. Mhlpfordt, T. Faulwasser, L. Roald, and V. Hagenmeyer, "Solving optimal power flow with non-gaussian uncertainties via polynomial chaos expansion," in *Proc. IEEE 56th Annu. Conf. Decis. Control*, Dec. 2017, pp. 4490–4496.
[16] B. N. Khoromskij and C. Schwab, "Tensor-structured Galerkin approximation of parametric and stochastic elliptic PDEs," *SIAM J. Sci. Comput.*, vol. 33, no. 1, pp. 364–385, 2011.
[17] D. Xiu, "Fast numerical methods for stochastic computations: A review," *Commun. Comput. Phys.*, vol. 5, no. 2–4, pp. 242–272, 2009.
[18] J. Peng, J. Hampton, and A. Doostan, "A weighted $l1$-minimization approach for sparse polynomial chaos expansions," *J. Comput. Phys.*, vol. 267, pp. 92–111, 2014.
[19] P. Chen and A. Quarteroni, "A new algorithm for high-dimensional uncertainty quantification based on dimension-adaptive sparse grid approximation and reduced basis methods," *J. Comput. Phys.*, vol. 298, pp. 176–193, 2015.
[20] T. G. Kolda and B. W. Bader, "Tensor decompositions and applications," *SIAM Rev.*, vol. 51, no. 3, pp. 455–500, 2009.
[21] J. Hampton and A. Doostan, "Compressive sampling of polynomial chaos expansions: Convergence analysis and sampling strategies," *J. Comput. Phys.*, vol. 280, pp. 363–386, 2015.
[22] B. Adcock, S. Brugiapaglia, and C. G. Webster, "Compressed sensing approaches for polynomial approximation of high-dimensional functions," in *Proc. Compressed Sens. Appl*. Springer, 2017, pp. 93–124.
[23] J. D. Jakeman, M. S. Eldred, and K. Sargsyan, "Enhancing $l1$-minimization estimates of polynomial chaos expansions using basis selection," *J. Comput. Phys.*, vol. 289, pp. 18–34, 2015.
[24] J. Li, H. Xin, W. Wei, and W. Dai, "Decentralised conic optimisation of reactive power considering uncertainty of renewable energy sources," *IET Renewable Power Gener.*, vol. 10, no. 9, pp. 1348–1355, 2016.
[25] H. Bludszuweit, J. A. Dominguez-Navarro, and A. Llombart, "Statistical analysis of wind power forecast error," *IEEE Trans. Power Syst.*, vol. 23, no. 3, pp. 983–991, 2008.
[26] X. He, L. Jiang, and W. Xia, "A stochastic model reduction method for nonlinear unconfined flow with multiple random input fields," *Stochastic Environmental Res. Risk Assessment*, vol. 31, no. 4, pp. 835–851, May 2017.
[27] K. Bruninx and E. Delarue, "A statistical description of the error on wind power forecasts for probabilistic reserve sizing," *IEEE Trans. Sustain. Energy*, vol. 5, no. 3, pp. 995–1002, Jul. 2014.
[28] U. Focken, M. Lange, K. Mnnich, H.-P. Waldl, H. G. Beyer, and A. Luig, "Short-term prediction of the aggregated power output of wind farms-a statistical analysis of the reduction of the prediction error by spatial smoothing effects," *J. Wind Eng. Ind. Aerodynamics*, vol. 90, no. 3, pp. 231–246, 2002.
[29] F. Bouffard and F. D. Galiana, "Stochastic security for operations planning with significant wind power generation," *IEEE Trans. Power Syst.*, vol. 23, no. 2, pp. 306–316, May 2008.
[30] P. Sarma, L. J. Durlofsky, and K. Aziz, "Kernel principal component analysis for efficient, differentiable parameterization of multipoint geostatistics," *Math. Geosci.*, vol. 40, no. 1, pp. 3–32, Jan. 2008.
[31] H. Kim and M. D. Shields, "Modeling strongly non-gaussian nonstationary stochastic processes using the iterative translation approximation method and Karhunen Leove expansion," *Comput. Structures*, vol. 161, pp. 31–42, 2015.
[32] O. G. Ernst, A. Mugler, H.-J. Starkloff, and E. Ullmann, "On the convergence of generalized polynomial chaos expansions," *ESAIM, Math. Model. Numer. Anal.*, vol. 46, no. 2, 2012, Art. no. 317C339.
[33] M. Farivar and S. H. Low, "Branch flow model: Relaxations and convexification," in *Proc. IEEE 51st IEEE Conf. Decis. Control*, Dec. 2012, pp. 3672–3679.
[34] L. Gan, N. Li, U. Topcu, and S. H. Low, "Exact convex relaxation of optimal power flow in radial networks," *IEEE Trans. Autom. Control*, vol. 60, no. 1, pp. 72–87, Jan. 2015.
[35] L. Gan, N. Li, U. Topcu, and S. Low, "On the exactness of convex relaxation for optimal power flow in tree networks," in *Proc. IEEE 51st IEEE Conf. Decis. Control*, Dec. 2012, pp. 465–471.
[36] E. DallAnese, K. Baker, and T. Summers, "Chance-constrained ac optimal power flow for distribution systems with renewables," *IEEE Trans. Power Syst.*, vol. 32, no. 5, pp. 3427–3438, Sep. 2017.
[37] J. Schmidli, L. Roald, S. Chatzivasileiadis, and G. Andersson, "Stochastic ac optimal power flow with approximate chance-constraints," in *Proc. Power Energy Soc. Gen. Meeting*, 2016, pp. 1–5.
[38] L. Roald, F. Oldewurtel, B. V. Parys, and G. Andersson, "Security constrained optimal power flow with distributionally robust chance constraints," unpublished paper, 2015. [Online]. Available: https://arxiv.org/abs/1508.06061
[39] A. Bruckstein, D. Donoho, and M. Elad, "From sparse solutions of systems of equations to sparse modeling of signals and images," *SIAM Rev.*, vol. 51, no. 1, pp. 34–81, 2009.
[40] A. Doostan and H. Owhadi, "A non-adapted sparse approximation of PDEs with stochastic inputs," *J. Comput. Phys.*, vol. 230, no. 8, pp. 3015–3034, 2011.
[41] M. Zhu and S. Martinez, "On distributed convex optimization under inequality and equality constraints," *IEEE Trans. Autom. Control*, vol. 57, no. 1, pp. 151–164, Jan. 2012.
[42] J. Li, H. Xin, W. Wei, and W. Dai, "Communication-efficient distributed strategy for reactive power optimisation considering the uncertainty of renewable generation," *IET Gener., Transmiss. Distrib.*, vol. 10, pp. 3681–3690, Nov. 2016.
[43] A. M. Bruckstein, D. L. Donoho, and M. Elad, "From sparse solutions of systems of equations to sparse modeling of signals and images," *SIAM Rev.*, vol. 51, no. 1, pp. 34–81, 2009.
[44] J. Li, W. Wei, and J. Xiang, "A simple sizing algorithm for stand-alone PV/wind/battery hybrid microgrids," *Energies*, vol. 5, no. 12, pp. 5307–5323, 2012.

Jing Li received the Ph.D. degree in control theory and control engineering from Zhejiang University, Hangzhou, China, in 2014. She is currently a Distinguished Research Fellow with the Zhejiang University City College, Hangzhou, China. Before that she was an Associate Professor with the Department of Information and Electronic Engineering, Zhejiang Gongshang University, Hangzhou, China.

Her research is currently working on optimizing operation of power system considering uncertainty, distributed optimization for distributed generators.

Na Ou is currently working toward the Ph.D. degree with the College of Mathematics and Econometrics, Hunan University, Changsha, China. Her research interests include uncertainty quantification and its applications to power system.

Guang Lin received the M.S. and Ph.D. degrees in applied mathematics from Brown University, Providence, RI, USA, in 2004 and 2007, respectively. He is currently an Associate Professor of mathematics and an Associate Professor of mechanical engineering, Purdue University, West Lafayette, IN, USA.

He has had in-depth involvement in developing uncertainty quantification tools for a large variety of domains including energy and environment. His research interests include diverse topics in computational science both on algorithms and applications, uncertainty quantification, and large-scale data analysis.

Wei Wei received the B.Eng., M.Eng., and D.Eng. degrees from the Zhejiang University, Hangzhou, China, in 1983, 1986, and 1994, respectively. He is currently a President with Zhejiang University City college and a Professor with Zhejiang University.

His current research interests include intelligent control and the development of novel technology of renewable energy and smart grid.